Ocean Dynamics (2013) 63:1113–1121
DOI 10.1007/s10236-013-0641-1

Surface charge distribution and its impact on interactions between sediment particles

Ming-hong Chen · Hong-wei Fang · Lei Huang

Received: 29 February 2012 / Accepted: 25 June 2013 / Published online: 20 July 2013

Abstract Surface charge distribution has great impact on interactions between sediment particles, which is essential for flocculation studies. In this paper, the micro-morphology and surface charge distribution of quartz sand are measured using the electrical force microscope. Then, the statistical relationship between micro-morphology and surface charge distribution is obtained. Results show that quartz sand possesses a complex surface morphology, which has great impact on the charge distribution. Positive and negative charges mostly concentrate in the saddle, convex, and concave parts of the surface, while their distribution is less in the groove, ridge, and flat parts. A fitting equation between surface charge and non-spherical curvature is also obtained. The surface charge distribution on a mathematical sediment particle is then reproduced according to these relations, and the effect of charge heterogeneity on interactions between different particles is quantified and analyzed, indicating that surface charge distribution has a dramatic effect on interactions between sediment particles, and local surface potential is more important than the average surface potential. This study provides a new method for understanding the processes of flocculation in coastal and estuarine zones.

Responsible Editor: Andrew James Manning

This article is part of the Topical Collection on the *11th International Conference on Cohesive Sediment Transport*

M.-h. Chen
College of Water Resources and Civil Engineering,
China Agricultural University, Beijing 100083, China
e-mail: chenminghong@cau.edu.cn

H.-w. Fang (✉) · L. Huang
Department of Hydraulic Engineering, the State Key Laboratory of Hydro-science and Engineering, Tsinghua University, Beijing 100084, China
e-mail: fanghw@mail.tsinghua.edu.cn

L. Huang
e-mail: huangl05@mails.tsinghua.edu.cn

Keywords Sediment particles · Surface charge · Micro-morphology · Interactions

1 Introduction

With the rapid development of the social economy, agricultural nonpoint source pollution and industrial point source pollution have led to serious river pollution in recent years. Strong physical, chemical, and biological interactions occur between sediment particles and contaminants, which greatly influence sediment surface properties. Flocculation of sediment in natural and engineered systems is still a subject of debate and utmost concern. Complex factors such as surface roughness, surface charge, and surface potential make it difficult to give a clear interpretation of this phenomenon (Taboada-Serrano et al. 2005).

Surface charge properties have great impact on interactions between sediment particles. Sediment in water acquires surface charge in many ways. Stumm (1992) figured that solid particle surfaces could develop an electrical charge by three principal means: (1) chemical reactions at the surface, (2) lattice imperfections and isomorphous replacement, and (3) adsorption of a hydrophobic species or a surfactant ion. Experiments on the measurement of sediment charge density have been addressed (Wang et al. 1997; Tang et al. 2000; Borgnino et al. 2006). These determined the average charge state mainly based on electrokinetic phenomena such as electrophoresis, electroosmosis, sedimentation, electroviscous flow, etc., or titration (Yin and Drelich 2008; Tan et al. 2005).

However, complex surface characteristics such as crystalline structure, mineral composition, and surface roughness always result in non-uniform charge distribution, which plays a key role in the behavior of sediment particles in the aquatic environment. So the direct observation of surface charge distribution is essential for flocculation study. Feick et al. (2000) used translational electrophoresis and electrophoretic rotation

to measure the average value and standard deviation of zeta potential on colloidal particles, respectively. Taboada-Serrano et al. (2005) measured surface charge heterogeneity of a silica plate by measuring a 2D array of force-versus-distance curves in electrolyte solutions via atomic force microscopy (AFM). Yin's group (2008) proposed a new technique, surface charge microscopy and measured the charge distribution of a multi-phase volcanic rock, especially across the boundary between adjacent phases. The bitumen–water interface was also studied (Drelich et al. 2007). However, direct measurement of the surface charge distribution of sediment has rarely been reported.

The stability of a colloidal system is mostly described by the Derjaguin–Landau–Verwey–Overbeek (DLVO) theory based on the electrical double-layer (EDL) structure, as shown in Fig. 1a (Taboada-Serrano 2005). It is assumed that the particle is a symmetrical sphere with a smooth surface and uniform charge distribution. For natural sediment particles, there are many complex micro-structures and pores of various scales on the surface. So a similar EDL structure can be supposed for these particles as shown in Fig. 1b. In contrast to the DLVO theory, surface roughness results in selective ion adsorption on the surface. The charge may concentrate in some regions, and excessive adsorption would even cause charge reversal (Taboada-Serrano et al. 2005). Based on this EDL structure, the classical theory could be modified to describe the behavior of sediment particles in aquatic environment more exactly.

A number of studies have been carried out to calculate the interactions between heterogeneously charged particles. Numerical methods, such as boundary element or finite difference techniques, are widely used (Grant and Saville 1995; Carnie et al. 1994). These methods can attain any desired accuracy, whereas they require a significant amount of numerical computation. Therefore, simple analytical formula would be more useful. Based on the Hogg–Healy–Fuerstenau model (Hogg et al. 1966), Velegol and Thwar (2001) proposed an analytical model for the effect of charge heterogeneity on colloidal interactions. Sennato et al. (2009) analyzed the interparticle potential of a liposome using Velegol's model and described the formation of large equilibrium aggregates. However, this model characterizes charge heterogeneity with only the average value and standard derivation of surface potential. Much detailed information is ignored. Sader et al. (1998) presented another analytical model expressed in terms of the moments of surface charge distribution and compared with the results of boundary element method. This model is based on the superposition approximation and can calculate interactions between two spheres with embedded point charges, which satisfy our need of the interaction calculation in this paper. However, these studies are mostly based on unreal charge distribution.

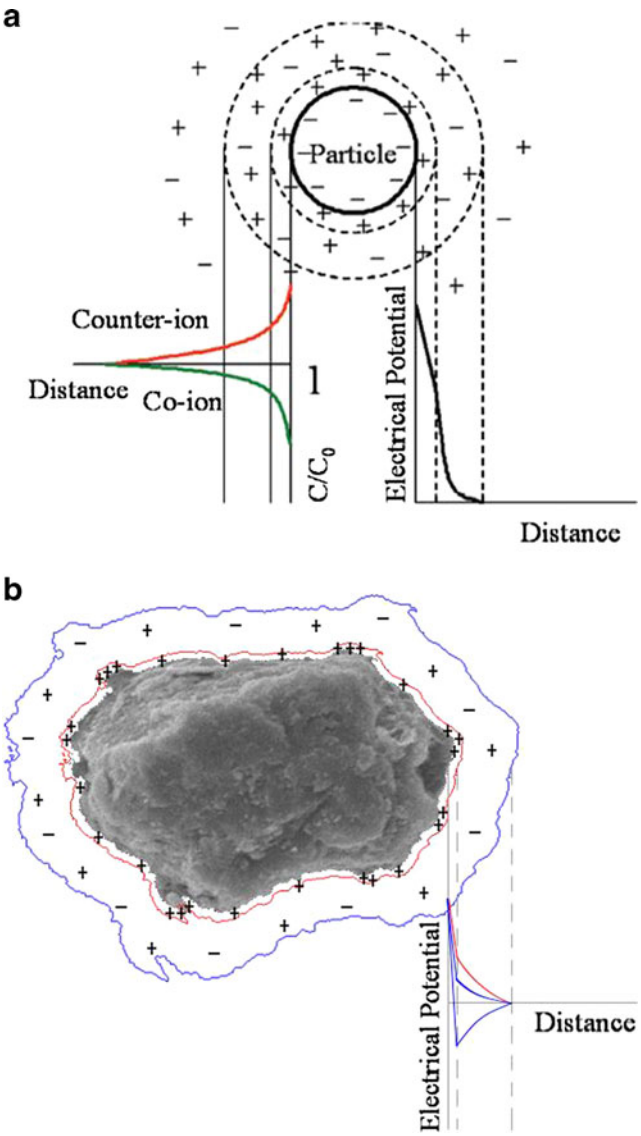

Fig. 1 Electrical double-layer structure for **a** the ideal particle (Taboada-Serrano 2005) and **b** natural sediment

Quartz is an important composition of sediment. For ease of measurement, quartz sand was taken as an example in this paper to measure its micro-morphology and surface charge distribution. The charge heterogeneity due to surface roughness was studied by analyzing the relations between surface charge distribution and micro-morphology. The surface charge distribution on a mathematical sediment particle is then reproduced according to these relations, and the effect of charge heterogeneity on the interaction free energy between two mathematical sediment particles is estimated using Sader's model. These studies enhance our understanding of surface charge distribution and its impact on interactions between sediment particles, providing a foundation for further flocculation study at a micro-level.

2 Experiment

The experimental method and the working principle of measuring instruments have been explicitly described by Huang et al. (2012). Here, only a brief introduction is given. Quartz sands were collected from natural rivers with a size range of 0.3~0.5 mm and stored in a clean glass dish. Experiments were completed by using a DI 3100 atomic force microscope in the Department of Physics at Tsinghua University.

The surface morphology image was obtained by DI300 using a contact mode in ambient conditions. The scanning range is 10 μm×10 μm, and the storage array is 256×256. Surface charge distribution was measured by the electrical force microscope (EFM) with a phase mode (Han 1999; Yang and Tang 2005; Dianoux et al. 2003; Zhao et al. 2007), and a phase image was subsequently obtained. The phase image shows the phase angle shift ($\Delta\varnothing_0$, hereafter referred to as phase shift) between the piezoelectric actuator driving signal and actual cantilever oscillation (Li et al. 2006), which is in proportion to surface charge. So the phase image provides a map of charge distribution on the sample surface (Huang et al. 2012; Magonov et al. 1997). The phase shift is positive when the electrostatic force acting on the tip is repulsive and negative when the force is attractive. Particularly, the greater the phase shift is, the greater the charge density is.

2.1 Surface morphology

Figure 2 is the morphology image of quartz sand obtained by AFM, which shows the morphology characteristic in nanoscale. The left is the top view, and the right is the 3D image. Brighter regions imply higher elevation. Units of the *x*- and *y*-axes are both micrometers. Surface elevation difference is up to 300 nm. The superiority of an AFM image is that it not only has a high resolution, but also can directly give the surface height of quartz sand, providing convenience for data analysis. It can be concluded from these pictures that quartz sands have extremely complex morphology, which may greatly impact charge distribution (Huang et al. 2012).

2.2 Surface charge distribution

Figure 3 shows the results of EFM measurement with a scanning range of 5.0 μm×2.5 μm and a storage array of 256×128. The distance between different scanning points is about 20 nm, providing a detailed description of surface morphology and charge distribution of quartz sand. The left one is a morphology image, in which bright regions and dark regions imply high and low elevation, respectively. The right one is the corresponding phase image, where bright regions represent positive phase shift, implying repulsive electrostatic force acting on the tip. In contrast, dark regions represent negative phase shift, implying an attractive electrostatic force is acting on the tip. The sign of the phase shift characterizes the sign of the charge while the magnitude of the phase shift can determine the strength of charge.

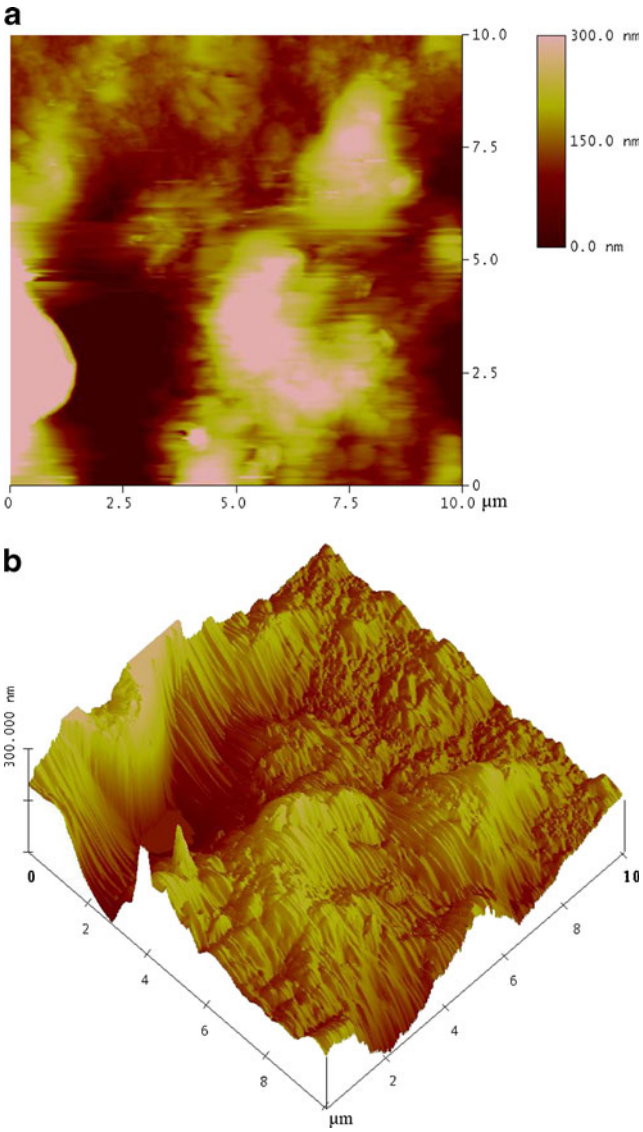

Fig. 2 **a**, **b** AFM images of quartz sand

The right phase image was obtained when a +5 V bias voltage was applied to the conductive tip. As stated above, the bright regions imply positive phase shift and repulsive force acting on the tip, so charge distributed in these regions should be positive, and brighter regions imply stronger positive charge. In contrast, dark regions imply negative phase shift and attractive force acting on the tip, so the charge there should be negative, and darker regions imply stronger negative charge. The existence of both bright regions and dark regions in the phase image implies that both positively charged

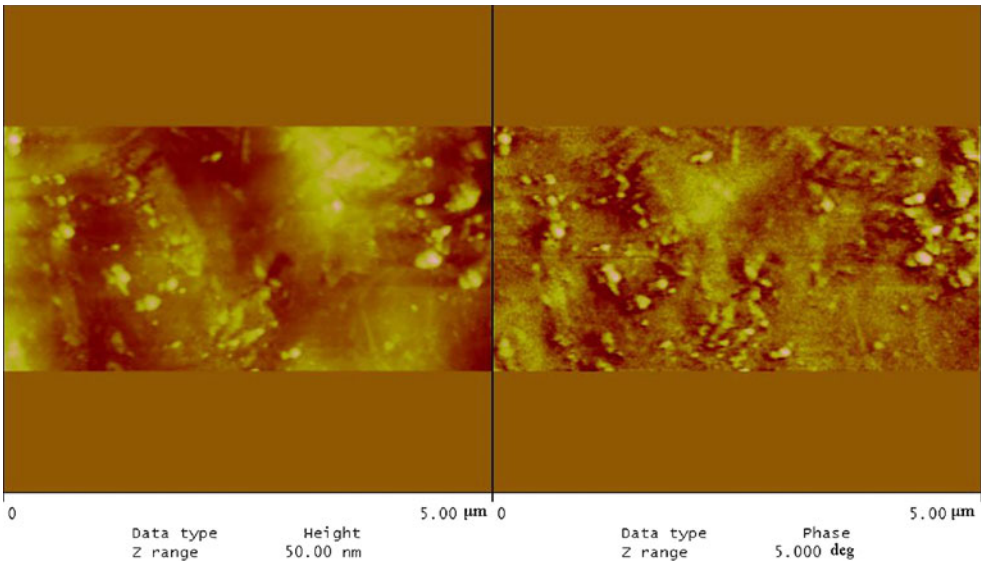

Fig. 3 Surface morphology (*left*) and phase image (*right*) of quartz sand

and negatively charged regions exist on the surface of quartz sand. It can be concluded that surface charge distribution has a strong correlation with morphology comparing the right phase image and the left morphology image. Regions with more complex morphology have a greater charge density. When no bias voltage was applied on the tip, only few information of charge distribution was obtained. When −5 V bias voltage was applied, a similar conclusion to that of +5 V bias voltage was drawn.

2.3 Statistical analysis of charge distribution and morphology

To further analyze the relations between charge distribution and micro-morphology, a statistical analysis is conducted. A similar analysis has been done in our previous study (Huang et al. 2012), and the conclusion is directly referenced here. Particle surfaces are classified into concave, convex, groove, ridge, flat, and saddle parts according to the local value of Gaussian curvature K and mean curvature H (Fang et al. 2009). Two groups of quartz sands (more than 100 particles in each group) are chosen for the analysis. For each particle, at least three different positions are observed to enhance the representativeness. Statistical analyses show that positive and negative charges mostly concentrate in the saddle, convex, and concave parts of the surface, with percentages of 53.26, 22.80, and 22.03 %, respectively, while their distribution is less in the groove, ridge, and flat parts.

Furthermore, the relation between surface charge and non-spherical curvature T is analyzed. Non-spherical curvature is defined as (Chen 2008)

$$T = \frac{1}{2}(k_1 - k_2) \tag{1}$$

where k_1 and k_2 are the principal curvatures, namely the maximum curvature and minimum curvature, respectively. On the surface of a sphere, the maximum curvature and minimum curvature are always equal, so $T=0$ at every position. A greater non-spherical curvature implies more complex morphology. To eliminate the impact of particle size and improve the universality, the curvature is normalized by dividing by the maximum value of T. Statistical analyses show that surface charge corresponds well with non-spherical curvature, and the fitting result is

$$\Delta\phi_0 = \mathrm{sgn}\left(q_{\mathrm{tip}}\right)\cdot\left(0.20 + 0.27e^{-15.06T} - 0.38e^{-1.80T}\right) \tag{2}$$

where q_{tip} is the surface charge of the tip. The sign function is defined as

$$\mathrm{sgn}\left(q_{\mathrm{tip}}\right) = \begin{cases} -1 & ; \quad q_{\mathrm{tip}} < 0 \\ 0 & ; \quad q_{\mathrm{tip}} = 0 \\ 1 & ; \quad q_{\mathrm{tip}} > 0 \end{cases} \tag{3}$$

The sign of phase shift changes with the sign of q_{tip}. However, for the surface charge of the particle, it does not depend on the sign of q_{tip}. The same results will be obtained no matter if positive or negative bias voltage is applied. Equation (2) represents the impact of surface morphology on the charge distribution. Combined with the calculation of non-spherical curvature, the charge distribution on the particle surface can be estimated.

3 Calculation

The traditional approaches to sediment transport calculations assume the particle to be a sphere, which is reasonable and feasible to a certain extent. However, with the increasing requirement of understanding the chemical transport and

biological transport, the studies on geometry and surface morphology of sediment particles become increasingly important. Fang's group (2009) is devoted to the development of a research platform of mathematical sediment analyses, using mathematical equations to characterize the geometry and surface morphology of sediment. They observe numerous natural sediment particles using a scanning electron microscope and establish a sample space by combining a large number of sediment particle profiles. Each profile corresponds to a mathematical equation. New profiles thus can be randomly generated using the distribution law of the sample space, and different profiles can be combined at different angles to reconstruct a 3D sediment particle. This particle is a mathematical sediment particle in a statistical sense. Figure 4 shows a generated mathematical sediment particle with a radius of 10 μm (the median size of the sediment particles in the Yangtze River, China). In this section, the previous conclusion is cited to reproduce the surface charge distribution of a mathematical sediment particle, and the effect of charge heterogeneity on interactions between different particles is analyzed.

3.1 Surface charge distribution of mathematical sediment particles

In theory, any complex surface can be approximated to arbitrary accuracy with high-order polynomials (Mei and Huang 2008). Also, the surface morphology of sediment particles can be described with quadratic polynomials. Due to the discontinuity of surface morphology, the block processing method is used. Suppose each point on the surface with eight surrounding neighborhood points form a micro-surface. Based on the theory of surface in differential geometry (Tang et al. 2005), the surface equation is set as $Z=Z\ (x, y)$, where x, y represents the coordinates in the image matrix. So the Gaussian curvature K and mean curvature H can be calculated using the following relations:

$$\begin{cases} K = k_1 k_2 = \dfrac{rt-s^2}{(1+p^2+q^2)^2} \\ H = \dfrac{k_1+k_2}{2} = \dfrac{(1+q^2)r-2pqs+(1+p^2)t}{2(1+p^2+q^2)^{3/2}} \end{cases} \tag{4}$$

where the physical meanings of p, q, r, s, and t are shown in Fig. 5. The elevation values $Z(x, y)$ can be directly obtained by the generated mathematical sediment particle, which is an $M\times N$ matrix. Using K and H, the non-spherical curvature is formulated as:

$$T = \frac{1}{2}(k_1-k_2) = \sqrt{H^2-K} \tag{5}$$

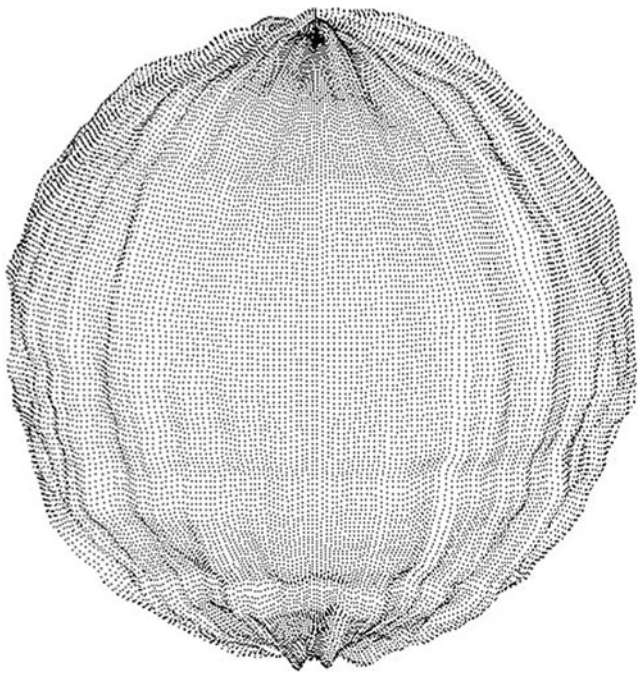

Fig. 4 Mathematical sediment (Fang et al. 2009)

For the mathematical sediment particle in Fig. 4, its surface charge distribution is reproduced with the scale of nanometer by applying the distribution law of Eq. (2) after the calculation of non-spherical curvature. Then, average calculation is carried out for the convenience of calculation. Figure 6 shows the top view of the surface charge distribution on the particle after local averaging. The surface is divided into several regions with a length scale of L, which cannot be too large in order to ensure accuracy. Here, the length scale of each region is 1 μm×1 μm. Each region is uniformly charged, and variances between different regions are expressed by different gray values.

It can be seen from Fig. 6 that the reproduced charge distribution of mathematical sediment is non-uniform, and both positive and negative charges exist on the surface, which is consistent with our previous experimental results. So this paper provides a method for modeling the non-uniform charge distribution of sediment particles. After surface charge distribution is known, we can estimate the effect of charge heterogeneity on interactions between different particles.

3.2 Interactions between mathematical sediment particles

A superposition formula for the electrical interaction between two heterogeneously charged spherical particles is proposed by Sader et al. (1998), which is a simple analytical formula expressed in terms of the moments of the surface

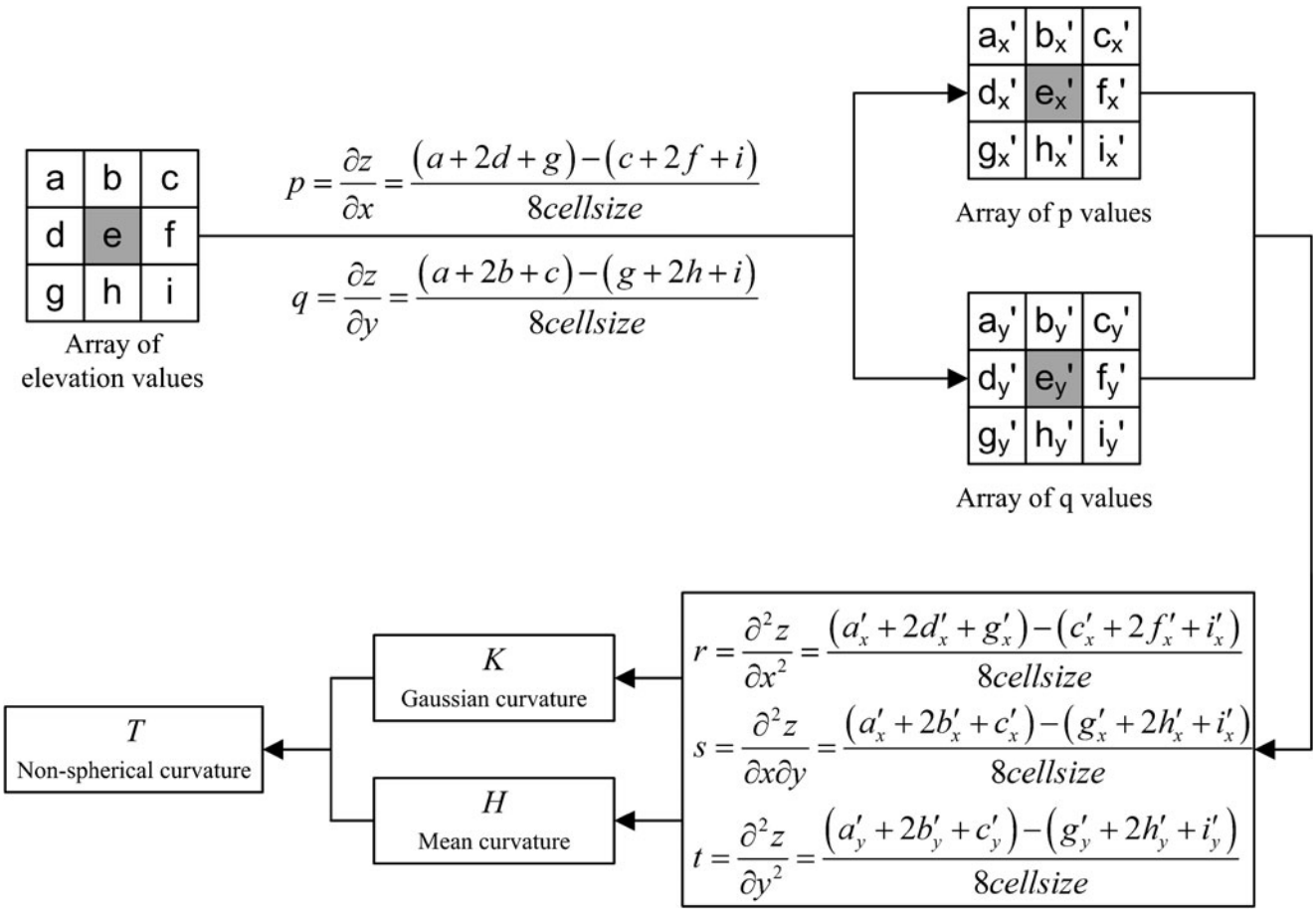

Fig. 5 Calculation flow chart of non-spherical curvature

charge distribution of each particle. In this section, the superposition formula is applied to calculate the interactions between mathematical sediment particles.

For the derivation, the electrical potential ψ_i throughout the electrolyte for a single particle is first required, which takes the well-known form (Kirkwood 1934)

$$\psi_i(r,\theta,\phi)=\sum_{n=0}^{\infty}\sum_{m=0}^{n}\left(\alpha_{m,n}\cos m\phi+\beta_{m,n}\sin m\phi\right)\frac{K_n(\kappa r)}{K_n(\kappa a)}\left(\frac{a}{r}\right)^{n+1}e^{-\kappa(r-a)}P_n^m(\cos\theta) \tag{6}$$

where a is the radius of the particle, (r, θ, ϕ) represents the position in the spherical coordinate system of the particle, $P_n^m(\cos\theta)$ are the associated Legendre functions (Abramowitz and Stegun 1972), and $K_n(x)$ is the Kirkwood function defined by

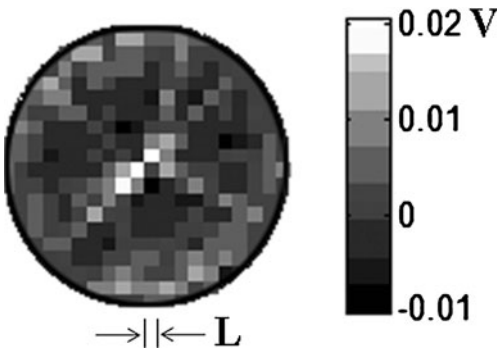

Fig. 6 Surface charge distribution of mathematical sediment particle

$$K_n(x)=\sum_{s=0}^{n}\frac{2^s n!(2n-s)!x^s}{s!(2n)!(n-s)!} \tag{7}$$

and the coefficients $\alpha_{m,n}$, $\beta_{m,n}$ are the moments of the surface charge distribution. In the case where the particle has a total of N discrete point charges imbedded in it, and each charge q_i is located at (r_i, θ_i, ϕ_i) in the spherical coordinate system of the particle, these moments can be calculated as follows:

$$\alpha_{m,n}=\frac{1}{4\pi\varepsilon_e a}\frac{(n-m)!}{(n+m)!}\frac{\sum_{i=1}^{N} q_i(r_i/a)^n P_n^m(\cos\theta_i)\cos m\phi_i}{\left[\frac{K_{n+1}(\kappa a)}{K_n(\kappa a)}-\frac{n}{2n+1}\left(1-\varepsilon_i/\varepsilon_e\right)\right]\gamma_m} \tag{8}$$

$$\beta_{m,n}=\frac{1}{2\pi\varepsilon_e a}\frac{(n-m)!}{(n+m)!}\frac{\sum_{i=1} q_i(r_i/a)^n P_n^m(\cos\theta_i)\sin m\phi_i}{\frac{K_{n+1}(\kappa a)}{K_n(\kappa a)}-\frac{n}{2n+1}\left(1-\varepsilon_i/\varepsilon_e\right)} \tag{9}$$

where ε_i and ε_e are the permittivities of the interior of the particle and of the electrolyte, respectively. γ_m equals 1 when $m=0$; otherwise, it equals 1/2. These moments are intimately related to the spherical coordinate system, so they may vary as the orientation of the particle is altered. Then, the electrical potential surrounding the two interacting particles is obtained by summing the individual contributions of the particles, that is

$$\psi=\psi_1+\psi_2 \tag{10}$$

Equation (10) is expected to be valid when the double layers of the two particles are weakly interacting. With the electrical potential throughout the electrolyte known, the interaction force between the two particles can be evaluated using the Maxwell stress tensor. And the interaction free energy ΔF then directly follows by integrating the force with respect to the separation between the particles.

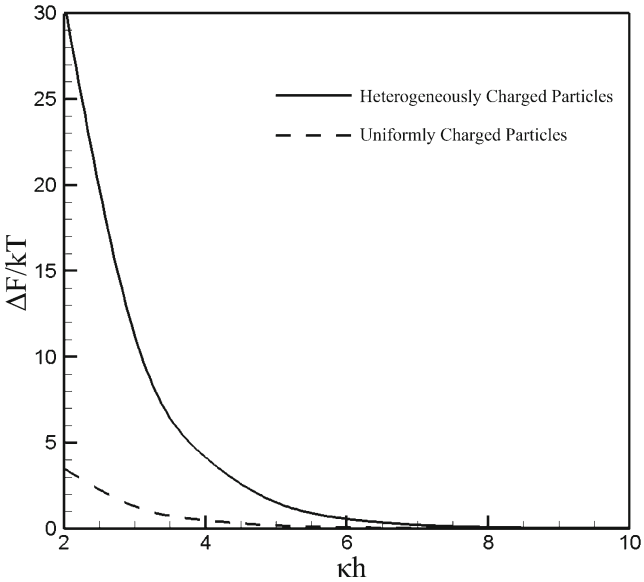

Fig. 7 Change of the interaction free energy with the separation between two particles

$$\Delta F=4\pi\varepsilon_e\frac{a_1a_2}{R}e^{-\kappa h}\sum_{n=0}^{\infty}\sum_{m=0}^{n}\sum_{\substack{i=0\\(i\le n-m)}}^{m}\frac{\gamma_m 2^{m-i}n!m!}{(n-m-i)!(m-i)!i!}\left(\frac{\Omega_{m,n-m-i}^{(A)}+\Omega_{m,n-m-i}^{(B)}}{(\kappa R)^n}\right) \tag{11}$$

where

$$\Omega_{m,n}^{(A)}=\sum_{i=0}^{n}\frac{n!}{(n-i)!i!}f_{m,m+i}^{(1)}f_{m,m+n-i}^{(2)},$$

$$\Omega_{m,n}^{(B)}=\sum_{i=0}^{n}\frac{n!}{(n-i)!i!}g_{m,m+i}^{(1)}g_{m,m+n-i}^{(2)},$$

$$f_{m,n}^{(s)}=\sum_{i=n}^{\infty}\frac{2^{(i-n)}i!(i+n)!}{(i-n)!(2i)!n!}\frac{(\kappa a_s)^i}{K_i(\kappa a_s)}\alpha_{m,i}^{(s)},$$

$$g_{m,n}^{(s)}=\begin{cases}\sum_{i=n}^{\infty}\frac{2^{(i-n)}i!(i+n)!}{(i-n)!(2i)!n!}\frac{(\kappa a_s)^i}{K_i(\kappa a_s)}\beta_{m,i}^{(s)}, & m\ge 1\\ 0 & \text{otherwise}\end{cases} \tag{12}$$

where $s=1, 2$ correspond to particles 1 and 2, respectively. R is the center-to-center distance between the particles, and h is their distance of closest approach, i.e., $h=R-a_1-a_2$.

Equation (11) is used to evaluate the interactions between two identical mathematical sediment particles, the surface charge distribution of which is reproduced in the previous

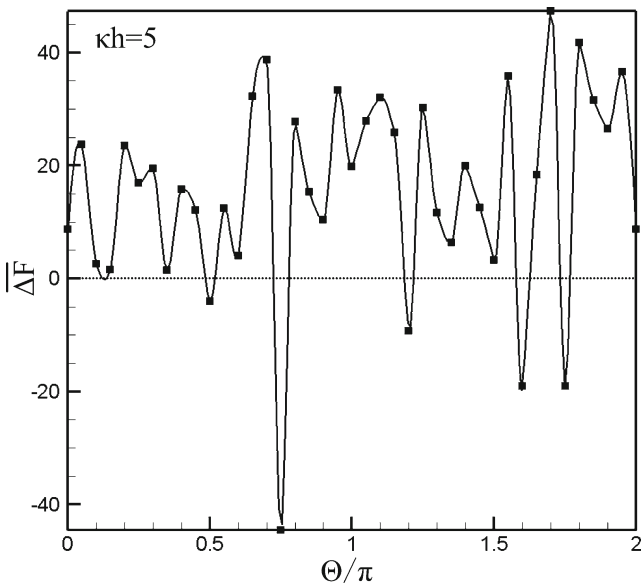

Fig. 8 Relations between the interaction free energy and the rotate angle with a fixed separation of $kh=5$

section and shown in Fig. 6. Statistics show that the particle takes an average surface potential of −1.55 mV, denoted as $\overline{\Phi}$.

Suppose there are two identical mathematical sediment particles with $a_1=a_2=10\ \mu m=10^{-5}m$ and $\overline{\Phi}_1=\overline{\Phi}_2=-1.55\,mV$. For pure water, $\varepsilon_e=\varepsilon_r\varepsilon_0=80\times8.85\times10^{-12}=7.08\times10^{-10}F/m$. The ratio of the permittivity of the electrolyte ε_e to that of the particle ε_i is taken to be 20. So $\kappa=\left(\frac{2e^2n_0Z^2}{\varepsilon_e kT}\right)^{1/2}=\left(\frac{2\times\left(1.6\times10^{-19}\right)^2\times6.02\times10^{24}}{7.08\times10^{-10}\times1.38\times10^{-23}\times300}\right)^{1/2}$,and Debye length κ^{-1}=3.08 nm.

Substituting the above parameters into Eq. (11), we can obtain the variation of the interaction free energy with the separation between two particles, kh, as shown in Fig. 7. The solid line represents the interaction free energy of the two identical mathematical sediment particles, and the dashed line is the results of two uniformly charged particles with surface potential of −1.55 mV, which is calculated by

$$\Delta F=4\pi\varepsilon_e\frac{a_1a_2}{R}\overline{\Phi}_1\overline{\Phi}_2e^{-\kappa h} \tag{13}$$

Results show that the interaction free energy decays rapidly with the separation and only survives in a few kh for both heterogeneously and uniformly charged particles. This can be easily found in Eqs. (11) and (13), which indicates that the interaction free energy would decay exponentially with the separation. However, for the case of heterogeneously charged particles, a much greater interaction free energy exists than the case of uniformly charged particles.

To further analyze the impact of surface charge distribution on interactions between sediment particles, a dynamic calculation is carried out. In the calculation, one particle is held stationary, and the other horizontally rotates an angle Θ, ranging from 0 to 2π. The variation of the orientation results in the change of the moments of the surface charge distribution, as discussed above. Then, the interaction free energy varies. Figure 8 shows the relations between the interaction free energy and the rotate angle with a fixed separation of kh=5. Here, ΔF is normalized by the interaction free energy of two uniformly charged particles, that is

$$\overline{\Delta F}=\frac{\Delta F}{4\pi\varepsilon_e(a_1a_2/R)\overline{\Phi}_1\overline{\Phi}_2e^{-\kappa h}} \tag{14}$$

For uniformly charged particles, $\overline{\Delta F}$ equals unity at any rotate angle. It can be seen from Fig. 8 that the interaction free energy varies greatly at different orientations with an average value of about 15. Particularly, it takes negative values at some rotate angles, which implies that attractive electrical interactions even exist between the two particles at some orientations. This calculation is a significant modification to the classical DLVO theory, indicating that surface charge distribution has a dramatic effect on interactions between sediment particles, and local surface potential is more important than the average surface potential.

4 Conclusion

In this paper, quartz sand is taken as an example to measure its micro-morphology and surface charge distribution with EFM, and analyze the statistical relations between them. Subsequently, surface charge distribution is reproduced on a mathematical sediment particle, and the effect of charge heterogeneity on the interaction free energy between two particles is estimated. Conclusions are drawn, as follows:

1. Quartz sand particles have extremely complex morphology which influences surface charge distribution greatly. Surface charge mostly concentrates in the saddle, convex, and concave parts of the surface, with percentages of 53.26, 22.80, and 22.03 %, respectively, while less distribution is found in the groove, ridge, and flat parts.
2. Both positively charged and negatively charged regions exist on the surface of quartz sand. Statistics show that surface charge corresponds well with non-spherical curvature.
3. The interaction free energy decays rapidly with the separation between two particles for both heterogeneously and uniformly charged particles. However, for the case of heterogeneously charged particles, a much greater interaction free energy exists than the case of uniformly charged particles.
4. The interaction free energy varies greatly with the orientation of sediment particles, and local surface potential is more important than the average surface potential.

Acknowledgments This research has been made possible with the support of the National Natural Science Foundation of China, grant no. 50909095, and Chinese Universities Scientific Fund, grant no. 2011JS131.

References

Abramowitz M, Stegun IA (1972) Handbook of mathematical functions. Dover, New York

Borgnino L, Avena M, De Pauli C (2006) Surface properties of sediments from two Argentinean reservoirs and the rate of phosphate release. Water Res 40:2659–2666

Carnie SL, Chan DYC, Stankovich J (1994) Computation of forces between spherical colloidal particles: nonlinear Poisson-Boltzmann theory. J Colloid Interface Sci 165:116–128

Chen ZH (2008) Experiment study on surface morphology and structural properties of sediment after copper ions adsorption. Dissertation, Tsinghua University

Dianoux R, Martins F, Marchi F (2003) Detection of electrostatic forces with an atomic force microscope: analytical and experimental

dynamic force curves in the nonlinear regime. Phys Rev B 68:045403–045408
Drelich J, Jun L, Yeung A (2007) Determining surface potential of the bitumen-water interface at nanoscale resolution using atomic force microscopy. Can J Chem Eng 85:625–634
Fang HW, Chen MH, Chen ZH (2009) Surface characteristics and model of environmental sediment. Science Press, Beijing
Feick JD, Velegol D (2000) Electrophoresis of spheroidal particles having a random distribution of zeta potential. Langmuir 16:10315–10321
Grant ML, Saville DA (1995) Electrostatic interactions between a nonuniformly charged sphere and a charged surface. J Colloid Interface Sci 171:35–45
Han L (1999) Nano fabrication using scanning probe microscope. Tsinghua University, Dissertation
Hogg R, Healy TW, Fuerstenau DW (1966) Mutual coagulation of colloidal dispersions. Trans Faraday Soc 62:1638–1651
Huang L, Fang HW, Chen MH (2012) Experiment on surface charge distribution of fine sediment. Sci China Ser E 55:1146–1152
Kirkwood JG (1934) Theory of solutions of molecules containing widely separated charges with special application to zwitterions. J Chem Res 2:351–361
Li Y, Qian JQ, Xu P et al (2006) Design and research of phase imaging-mode atomic force microscopy. J of Chin Electron Microsc Soc 25:341–344 (in Chinese)
Magonov SN, Elings V, Whangbo MH (1997) Phase imaging and stiffness in tapping-mode atomic force microscopy. Sur Sci 375:L385–L391
Mei XM, Huang JZ (2008) Differential geometry, 4th edn. Higher Education Press, Beijing
Sader JE, Lenhoff AM (1998) Electrical double-layer interaction between heterogeneously charged colloidal particles: a superposition formulation. J Colloid Interface Sci 201:233–243
Sennato S, Truzzolillo D, Bordi F et al (2009) Colloidal particle aggregates induced by particle surface charge heterogeneity. Colloid Surf A-Physicochem Eng Asp 343:34–42
Stumm W (1992) Chemistry of the solid-water interface. Wiley, New York
Taboada-Serrano P (2005) Colloidal interactions in aquatic environments: effect of heterogeneity and charge asymmetry. Dissertation, Georgia Institute of Technology
Taboada-Serrano P, Vithayaveroj V, Yiacoumi S, Tsouris C (2005) Surface charge heterogeneities measured by AFM. Environ Sci Technol 39:6352–6360
Tan SS, Robert LS, Qin DQ (2005) Surface heterogeneity of polystyrene latex particles determined by dynamic force microscopy. Langmuir 21:43–49
Tang HX, Qian Y, Wen XH (2000) Characteristics and control technologies of water particles and refractory organics. China Environmental Science Press, Beijing
Tang GA, Liu XJ, Yan GN (2005) Principles and methods of digital elevation models and ground analysis. Science Press, Beijing
Velegol D, Thwar PK (2001) Analytical model for the effect of surface charge nonuniformity on colloidal interactions. Langmuir 17:7687–7693
Wang FY, Chen JS, Chen JL (1997) Surface properties of natural aquatic sediments. Water Res 31:1796–1800
Yang YY, Tang HM (2005) Measurement of chitosan material surface charge distribution using scanning probe microscope. J Mater Sci Eng 23:605–608 (in Chinese)
Yin XH, Drelich J (2008) Surface charge microscopy: novel technique for mapping charge-mosaic surfaces in electrolyte solutions. Langmuir 24:8013–8020
Zhao HB, Han L, Wang XF (2007) A new measurement system based on EFM for charges on dielectric surface in micro-nanometre scale. Insulating Mater 40:66–68 (in Chinese)